J Mater Sci: Mater Electron

Effect of CeO_2 nanoparticles on dielectric properties of PVB/CeO_2 polymer nanodielectrics: a positron lifetime study

M. Raghavendra[1], K. Jagadish[2], S. Srikantaswamy[2], T. M. Pradeep[1], A. P. Gnana Prakash[1], and H. B. Ravikumar[1,*]

[1] Department of Studies in Physics, University of Mysore, Manasagangotri, Mysuru 570006, Karnataka, India
[2] Department of Studies in Environmental Science, University of Mysore, Manasagangotri, Mysuru 570006, Karnataka, India

Received: 31 August 2021
Accepted: 10 November 2021

ABSTRACT

To produce a polymer nanodielectric material with low dielectric constant for high speed communication network cables, polymer nanodielectrics of Polyvinyl butyral (PVB) with (0.2, 0.4, 0.6, 0.8, and 1 wt%) of CeO_2 nanoparticles are prepared. Cerium dioxide (CeO_2) nanoparticles were synthesized by hydrothermal technique. The average size of CeO_2 nanoparticles determined by Dynamic Light Scattering studies is 60 nm. The dependence of free volume and crystallinity on dielectric properties of PVB/CeO_2 polymer nanodielectrics is explored. The positron lifetime parameters viz., o-Ps lifetime (τ_3) and free volume size (V_f) show minimum value for 1.0 wt% of CeO_2 nanoparticles loading. The reduced free volume is attributed to the increased chemical interaction between CeO_2 nanoparticles and PVB side chain. The AC conductivity and dielectric constant of PVB/CeO_2 polymer nanodielectrics are also decreased for 1.0 wt% of CeO_2 nanoparticle loading. The reduced free volume restricts the ionic mobility of CeO_2 nanoparticles and impedes dipoles mobility.

1 Introduction

In recent times, the prospect of using polymer nanocomposites as dielectric materials for electrical insulation is gaining enormous attention [1]. Polymer nanodielectrics are basically consisted of polymers with an adjunct of inorganic nanofillers [2]. The bulk material properties of a polymer are very much influenced by the incorporated nanofiller. Consequently, the properties of the resulting composite may be more likely to resemble those of the interface zones rather than those of the original constituents [3]. The nanodielectrics interface plays a vital role in enhancing the bulk dielectric properties of polymer nanodielectrics.

It was previously reported that the presence of a polar group in the polymer matrix is more advantageous to tailor dielectric properties. The polarities of nanofillers play a significant role in the enhancement of dielectricity of polymer nanocomposites [4]. The

Address correspondence to E-mail: hbr@physics.uni-mysore.ac.in

https://doi.org/10.1007/s10854-021-07379-z
Published online: 22 November 2021

metal oxide nanoparticles are the better choice for the enhancement of dielectricity in the polymer nanodielectrics. They exhibit net negative surface charge and form strong ionic interactions with positively charged polymeric surfaces [5]. Because of their immense optical, thermal, and electrical properties, nanocrystalline rare-earth metal oxides got significant attention in the preparation of polymer nanodielectrics [6]. One such rare-earth metal oxide nanoparticle is Cerium dioxide (CeO_2). Cerium dioxide can easily adjust to the surface condition and exhibit stable structure far from the stoichiometric proportion of oxygen [7]

PVB is a highly amorphous terpolymer containing vinyl, butyl, and alcohol functional groups [8]. The polar components present in the PVB polymer can interact with dopant macromolecules [9]. In addition to that PVB polymer exhibits excellent film-forming ability and provides good adhesion to various surfaces [10]. PVB polymer is a good ceramic binder and is widely used in the automotive industries [11]. The studies on PVB-based polymer nanodielectrics with different types of nanofillers can be found in the literature [12–14]. However, the dependence of free volume on dielectric properties of PVB/CeO_2 polymer nanodielectrics are nowhere reported. Motivated by this, the authors are interested to carry out studies related to dependence of free volume and crystallinity on the dielectric behavior of PVB/CeO_2 polymer nanodielectrics. In the present investigation, Cerium dioxide (CeO_2) nanoparticles of about 60 nm size were synthesized by hydrothermal technique. The microstructural characterization of PVB/CeO_2 polymer nanodielectrics are performed by employing well-known nondestructive technique viz., Positron annihilation lifetime spectroscopy (PALS). In addition, the studies on surface morphology and crystallinity of polymer nanodielectrics have also been performed and the results were reported here.

2 Experimental

2.1 Materials

The Polyvinyl butyral (PVB) polymer used in the present study is purchased from Sigma-Aldrich, USA. The average molecular weight (M_w) of PVB polymer is 70,000 and density is 1.08 g/cm^3. Cerium dioxide (CeO_2) nanoparticles prepared by Hydrothermal method have particle diameter of 60 nm.

2.2 Synthesis of CeO_2 nanoparticles by hydrothermal method

The mixture of 0.1 mol of Cerium nitrate [$Ce(NO_3)_3{\cdot}6H_2O$] and 0.3 mol of Sodium hydroxide (NaOH) solutions was transferred to a 20 mL capacity Teflon liner. The Teflon liner was fixed with stainless steel autoclaves in the hot air oven. The mixture was heated in a hot air oven at 180 °C for 5 h and then cooled to room temperature. The product was centrifuged and washed three times with deionized water. The product was then dried at 80 °C for 5 h inside the hot air oven. The dried product was calcinated at 400 °C for 4 h in a muffle furnace to get the final product.

2.3 Preparation of polymer nanodielectrics

PVB/CeO_2 polymer nanodielectrics films were prepared by the usual solution casting technique. Initially, 5 g of PVB polymer was dissolved in 50 ml ethyl methyl ketone solvent and stirred well using a magnetic stirrer until the solution attains suitable viscosity. In another beaker, CeO_2 nanoparticles were dissolved using the same solvent and added to the polymeric solution. The mixture was heated at 40 °C for 2 h. The resulting mixture was then poured onto a clean glass mold and dried for 24 h. The prepared films of PVB/CeO_2 polymer nanodielectrics are about 1.0–2.0 mm thick. These films were cut into samples of 1.5 cm × 1.5 cm dimensions and kept in the desiccator for one week. The same samples are subjected to PALS, AC conductivity, dielectric, SEM, and XRD studies.

3 Measurements

3.1 Dynamic light scattering (DLS) studies

The average particle size of Cerium dioxide (CeO_2) nanoparticles was analyzed using the DLS instrument model (Microtrac-nanotrac wave-w 3231) at a scattering angle of 90° at room temperature). The pure solvent was used to make background correction and using zeta potential the size of dispersed nanoparticles was estimated.

3.2 Energy-dispersive X-ray (EDX) spectroscopy studies

The elemental composition of CeO_2 nanoparticles was done by making use of Elemental analyzer (EA; German Elementar Analysensysteme inc., D63452 Hanau).

3.3 Scanning electron microscopy studies

The SEM analysis of pure CeO_2 nanoparticles, PVB, and PVB/CeO_2 polymer nanodielectrics was done by making use of Scanning Electron Microscope (SEM) (model ZEISSEVO15, Germany) with the accelerating voltage of 15 kV. To obtain the SEM images, CeO_2 nanoparticles and PVB/CeO_2 polymer nanodielectric films were kept on the aluminum stubs. The aluminum stubs are coated with gold to avoid electrical charging during the examination. All SEM images were obtained at 5KX magnification.

3.4 X-ray diffraction studies

X-ray diffractograms of pure CeO_2 nanoparticles and PVB/CeO_2 polymer nanodielectric samples were taken using Rigaku MiniFlex 11 diffractometer with CuKα (1.5406 Å) radiation. The Ni filter and graphite monochromator are used to absorb K_β radiation and render the monochromatic radiation, respectively. The X-ray diffractograms were obtained from 5° to 60° in the 2θ range in steps of 0.02° with a scan speed of 5°/min. The voltage and current were maintained to be 0–60 kV and 0–80 mA, respectively. The crystallinity and crystallite size of PVB/CeO_2 polymer nanodielectrics are evaluated by the deconvolution of XRD spectra using PEAKFIT4.1 software.

3.5 Positron annihilation measurements

Positrons emanated from radioactive sources are very much sensitive to material mediums like polymer. It undergoes thermalization in the material medium, during which all its kinetic energy gets converted into thermal energy within a short time. Then, it finds an electron with the opposite spin and gets annihilated. Positron annihilation process involves different positron states viz., free annihilation; this would always correspond to a localized state (trapped state) or form a bound state. The bound state of positron and electron coexists with definite binding energy collectively called positronium (Ps). Ps can exhibit two spin states, namely para-positronium (p-Ps), which is always associated with antiparallel spin orientation annihilates with a lifetime of 0.125 ns. The ortho-positronium (o-Ps) having parallel spin orientation annihilates with a lifetime of 140 ns in free space. This process is called as o-Ps pick-off annihilation, in which the o-Ps lifetime gets reduced to a few nanoseconds. The relative abundance of these two states would be 1:3. Each of these annihilation processes has got a characteristic lifetime. The long-lived o-Ps has a finite probability of annihilating with an electron in the free volume site other than its bound partner. Therefore, o-Ps lifetime is considered an important parameter for the determination of free volume hole size in the polymer matrix [15].

In the present study, we have employed a fast–fast coincidence system with conically shaped BaF_2 scintillators coupled to photomultiplier tubes of type XP2020/Q with quartz windows as detectors. Two identical pieces of the samples were placed on either side of a 15 μCi–^{22}Na positron source deposited on a pure Kapton foil of 0.0127 mm thickness. This sample source sandwich was placed between the two detectors to acquire a lifetime spectrum. The coincidence lifetime spectrometer was operated at 280 Ps and all the lifetime measurements were performed at room temperature. Two to three positron lifetime spectra with more than a million counts under each spectrum were recorded in a time of 5–7 h [16]. Consistently reproducible spectra were analyzed into three lifetime components with the help of the computer program PATFIT-88 [17] with proper source and background corrections. The source correction term and resolution function were estimated from the lifetime of well-annealed aluminum using the program RESOLUTION [18]. The three Gaussian resolution functions were used in the present analysis of positron lifetime spectra of as-received PVB and PVB/CeO_2 polymer nanocomposites for different cerium dioxide concentrations. The o-Ps lifetime (τ_3) is related to the free volume hole size by a simple relation given by Nakanishi et al. [18] which was developed based on theoretical models originally proposed by Tao [19] for molecular liquids and later by Eldrup et al. [20]. In this model, positronium is assumed to be localized in a spherical potential well having an infinite potential barrier of radius 'R_0'with an electron layer in the region $R < r < R_0$. The

relation between 'τ_3'and the radius 'R' of the free volume hole or cavity is as follows.

$$\lambda = \frac{1}{\tau_3} = 2\left[1 - \left(\frac{R}{R_0}\right) + \left(\frac{1}{2\pi}\right)\mathrm{Sin}\left(\frac{2\pi R}{R_0}\right)\right]\mathrm{ns}^{-1} \quad (1)$$

where $R_0 = R + \delta R$ and δR is an adjustable parameter. By fitting Eq. (1) with 'τ_3' values for known hole sizes in porous materials, like zeolites, a value of $\delta R = 0.1657$ nm was obtained. With this value of δR, free volume radius 'R' has been calculated from Eq. (1) and the average size of free volume holes (V_f) is evaluated by

$$V_f = \frac{4}{3}\pi R^3 \quad (2)$$

The fractional free volume or the free volume content (F_v) can then be estimated by

$$F_\mathrm{v} = CV_\mathrm{f}I_3 \quad (3)$$

where 'C' is structural constant, whose value is taken as 0.0018 $\mathrm{Å}^{-3}$ [21], 'V_f' is the free volume hole size, and 'I_3' is the o-Ps intensity.

3.6 AC conductivity and dielectric measurements

The AC conductivity and dielectric parameters of PVB/CeO_2 polymer nanodielectrics having different CeO_2 nanoparticle concentrations (0.2 to 1.0 wt%) have been carried out using HIOKI 3532-50 Hi-tester (Japan) model. Both sides of PVB/CeO_2 polymer nanodielectrics samples were coated with a silver paste to ensure electrical contact. The PVB/CeO_2 polymer nanodielectric samples of dimensions (1.5 cm × 1.5 cm × 1 mm) were sandwiched between two electrodes. The conductance, tanδ, and capacitance data are recorded using an LCR meter in the frequency range 100 Hz to 5 MHz at room temperature. The AC conductivity of PVB/CeO_2 polymer nanodielectric films was evaluated using the relation

$$\sigma_\mathrm{ac} = \frac{Gd}{A}\mathrm{s/cm} \quad (4)$$

where 'G' is the conductance, 'd' is the thickness, and 'A' is the area of cross-section of the polymer nanodielectric sample. The dielectric constant (ε') and dielectric loss (ε'') of the material can be evaluated by the relations

$$\varepsilon' = \frac{Cd}{\varepsilon_0 A} \quad (5)$$

and

$$\varepsilon'' = \varepsilon' \tan\delta, \quad (6)$$

respectively, where 'C' is the capacitance, 'ε_0' is the permittivity of free space, and tanδ is the tangential loss.

4 Results and discussion

4.1 Dynamic light scattering (DLS) results

The advanced technique viz., DLS is used to deduce the size profile of small particles in the suspension or solutions in the science research [22]. The CeO_2 nanoparticle's size distribution obtained by the DLS study is as shown in Fig. 1. The nanoparticles with different sizes and concentrations are estimated using the DLS instrument. The size distribution of CeO_2 nanoparticles lies in the 10 to 90 nm range in the suspension. The maximum count is observed within (60 nm to 80 nm) range. The average size of CeO_2 nanoparticles was found to be 60 nm. The stability of CeO_2 nanoparticle suspension can also be accessed using DLS. The stability analysis of the CeO_2 nanoparticles is convenient to check the nanoparticle aggregate in the suspension.

4.2 Energy-dispersive X-ray (EDX) spectroscopy results

Energy-dispersive X-ray spectroscopy (EDX) is used to characterize the elemental composition of the chemical compounds on a micro- or nanoscale [23]. The EDX spectra of CeO_2 nanoparticles prepared by the hydrothermal method are as shown in Fig. 2. The added mass of pure ingredients and the final quantity of the obtained CeO_2 nanoparticles were compared during the preparation of CeO_2 nanoparticles. The inset table shows the amount of Oxygen (O) and Cerium contents in the synthesized CeO_2 nanoparticles. The CeO_2 nanoparticles are found to have 33.33% and 66.67% of Ce and O elements, respectively. The elemental composition of as-prepared CeO_2 nanoparticles determined by the EDX analysis is in close agreement with the calculated values.

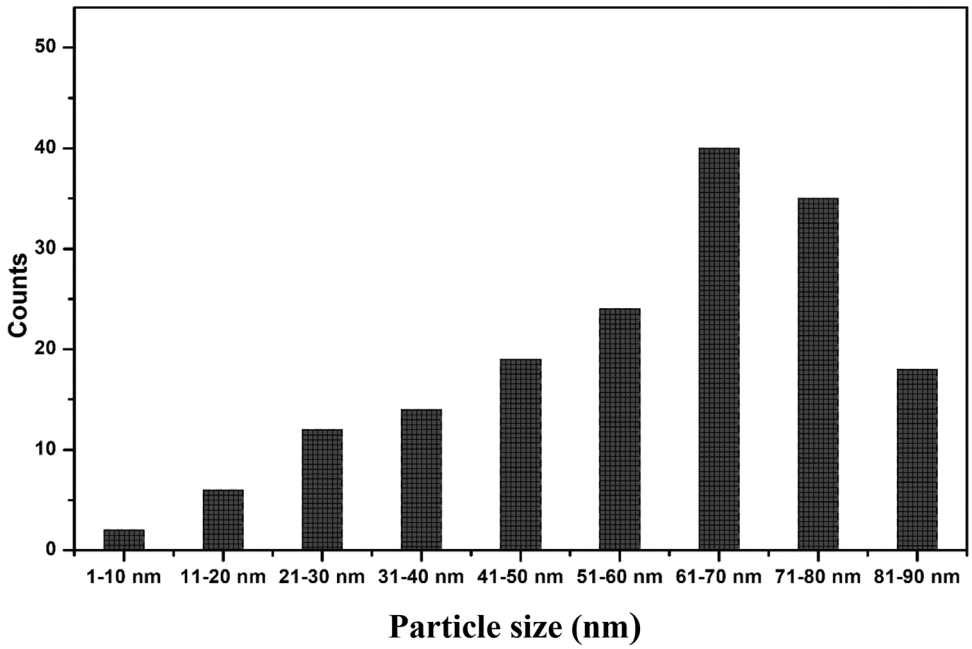

Fig. 1 Particle size distribution of CeO_2 nanoparticles synthesized by hydrothermal method

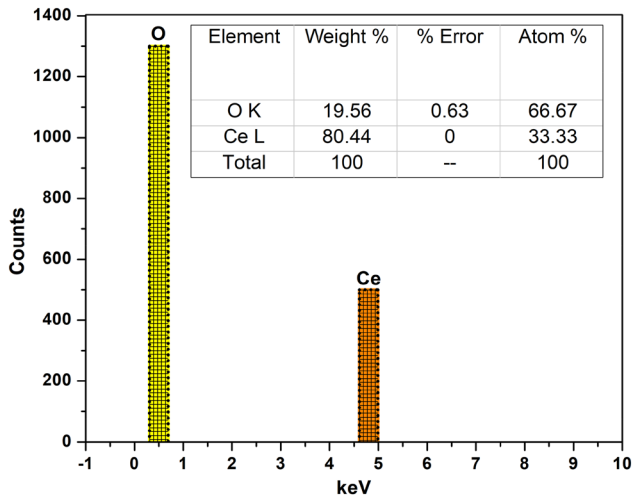

Fig. 2 EDX spectrum of CeO_2 nanoparticles synthesized by hydrothermal method

4.3 XRD results of Cerium dioxide (CeO_2) nanoparticles

The XRD patterns of the synthesized CeO_2 nanoparticle measured in the 2θ range from 10° to 80° are as shown in Fig. 3. The XRD spectrum of CeO_2 nanoparticle shows characteristic diffraction peaks at 2θ = 28.66, 33.03, 47.96, 56.39, and 79.27° which correspond to (111), (200), (220), (311), and (420) planes, respectively. The obtained reflections correspond to the face-centered cubic phase of the CeO_2 nanoparticle (JCPDS file No: 81-0792).

4.4 SEM results of cerium dioxide (CeO_2) nanoparticles

The morphology of various micro- and nanomaterials can be assessed using Scanning electron microscopy (SEM). The SEM images of synthesized cerium dioxide nanoparticles shown in Fig. 4a and b exhibit highly dense irregular structures [24]. It was reported in the literature that CeO_2 nanoparticles have a greater tendency to undergo self-agglomeration [25]. Therefore, the formation of highly dense irregular structure in the SEM images is attributed to the self-

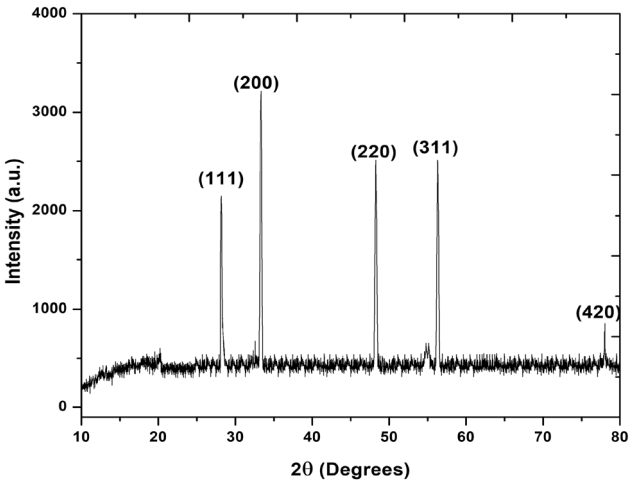

Fig. 3 XRD graph of CeO_2 nanoparticles synthesized by hydrothermal method

agglomeration of CeO_2 nanoparticles in the sample holder.

4.5 Positron lifetime results of PVB/CeO_2 polymer nanodielectrics

In this study, the author made an effort to evaluate the free volume hole size (V_f) and their concentrations in the pure PVB and PVB/CeO_2 polymer nanodielectrics. The third-lifetime component (τ_3) and its o-Ps intensity (I_3) that have been extracted from PATFIT-88 are tabulated in Table 1. The o-Ps lifetime (τ_3) and o-Ps intensity (I_3) of pure PVB obtained from the PATFIT-88 analysis of positron lifetime spectrum are 1.952 ± 0.009 ns and 29.04 ± 0.21%, respectively. The corresponding free volume hole size (V_f) for pure PVB derived using Eq. (1) is 93.13 ± 0.74 $Å^3$. Figure 5a and b displays the graphs of an o-Ps lifetime (τ_3), free volume hole size (V_f), and o-Ps intensity (I_3) as a function of CeO_2 nanofiller concentration. From Fig. 5a, it is observed that the o-Ps lifetime (τ_3) decreases linearly as a function of CeO_2 nanofiller concentration. There is about a 46 Ps reduction in the o-Ps lifetime (τ_3) for 0.4 wt% of CeO_2 nanoparticle loading compare to pure PVB polymer. This is reflected in the decrement of 4.30 $Å^3$ in the free volume size from 93.13 to 88.83 $Å^3$. A remarkable reduction of an o-Ps lifetime (τ_3) is observed for 0.8 and 1.0 wt% of CeO_2 nanofiller loading. This corresponds to 78 Ps and 112 Ps decrement in the o-Ps lifetime (τ_3) of PVB/CeO_2 polymer nanodielectrics for 0.8 and 1.0 wt% of CeO_2 nanofiller concentration, respectively. Consequently, there are about 7.25 $Å^3$ and 9.88 $Å^3$ decreases in the free volume size which is observed for 0.8 and 1.0 wt% of CeO_2 nanoparticle loading, respectively. The detailed interpretation for these changes can be given as follows.

It was previously reported that the free volume parameters provide better insight into the interfacial properties of polymer and nanocomposites. In semicrystalline polymers, o-Ps is preferentially annihilated from both densely packed crystalline phase and the holes in an amorphous phase [26]. In the case of fully amorphous polymers o-Ps is trapped and gets annihilated from the free volume sites [27]. However, in the polymer nanodielectrics the o-Ps formation predominantly takes place in the polymer–nanofiller interface [28]. Polymers are long-chain molecules and they can take different conformations in all possible directions. As the nanoparticles exhibit a large surface area, they can easily interact within the polymeric chain and impede the chain mobility of the host polymer [29].

The formation of covalent bond between Ce^{2+} ions of CeO_2 nanoparticles with carbonyl group of PVB side chain takes place [30]. The hydrogen bonding between O^- ions of CeO_2 nanoparticles and methyl group of PVB side chain cannot be ruled out [5]. The chemical interaction between Ce^{2+} and O^- ions of CeO_2 nanoparticles with PVB side chain hinders the molecular mobility of PVB polymer and hence the free volume [5]. The increased addition of CeO_2 nanoparticles may create oxygen-rich phase and deficient phase in the PVB matrix. This assumption is quite reasonable as CeO_2 nanoparticles possess oxygen vacancy site and rapid flipping of oxidation and reduction state (Ce^{3+} to Ce^{4+}) [31]. The phase with

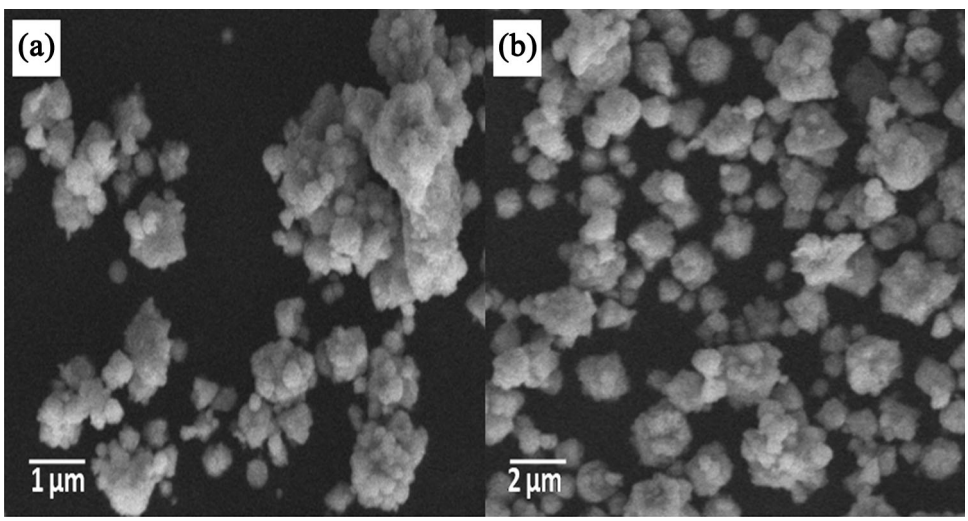

Fig. 4 SEM micrographs of CeO_2 nanoparticles synthesized by hydrothermal method. **a** 1 µm scale and **b** 2 µm scale

Table 1 PALS results of PVB/CeO_2 polymer nanodielectrics

WWt% of CeO_2 nanoparticle	o-Ps lifetime τ_3 (ns)	Free volume V_f (Å)^3	o-Ps intensity I_3 (%)	Fractional free volume F_v (%)
0.0	1.952 ± 0.009	93.13 ± 0.74	29.04 ± 0.21	1.88 ± 0.02
0.2	1.944 ± 0.009	92.34 ± 0.74	22.94 ± 0.17	1.47 ± 0.02
0.4	1.906 ± 0.009	88.83 ± 0.72	23.27 ± 0.18	1.43 ± 0.02
0.6	1.904 ± 0.008	88.64 ± 0.64	23.14 ± 0.16	1.42 ± 0.02
0.8	1.874 ± 0.010	85.88 ± 0.79	23.68 ± 0.22	1.41 ± 0.02
1.0	1.840 ± 0.008	83.25 ± 0.64	22.74 ± 0.15	1.39 ± 0.01

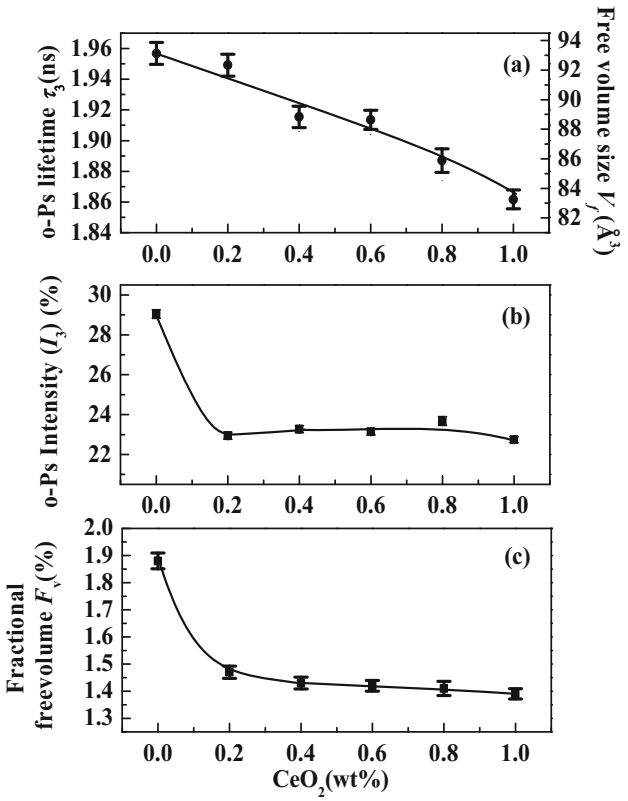

Fig. 5 Plot of free volume parameters **a** o-Ps lifetime (τ_3) and free volume hole size (V_f), **b** o-Ps intensity (I_3), and **c** fractional free volume (F_v) of PVB/CeO_2 polymer nanodielectrics as a function of CeO_2 nanoparticle wt%

effluent oxygen site may quench the o-Ps lifetime (τ_3). Consequently, the o-Ps lifetime (τ_3) of PVB/CeO_2 polymer nanodielectrics monotonically decreases upon the subsequent addition of CeO_2 nanoparticles.

The o-Ps intensity (I_3) conceptually represents the concentration or number density of free volume holes present in the polymeric system [32]. Figure 5b shows the plot of o-Ps intensity (I_3) of PVB/CeO_2 polymer nanodielectrics as a function of CeO_2 nanoparticle concentration. The o-Ps intensity (I_3) decreases to 22.94% from 29.04% for 0.2 wt% of CeO_2 nanoparticle loading. Initially, the CeO_2 nanoparticles were uniformly distributed over a certain fraction of the PVB polymer surface. The polar groups of the PVB matrix may inhibit the o-Ps formation probability. Consequently, o-Ps intensity (I_3) is reduced for 0.2 wt% of CeO_2 nanofiller loading. The o-Ps intensity (I_3) value fluctuates within the error limits and becomes constant for higher wt% of CeO_2 nanoparticle loading. The polar groups of CeO_2 nanoparticles in the host PVB matrix act as Ps inhibitors [33]. This is due to the agglomeration of CeO_2 nanoparticles in the PVB matrix [34]. The variation of fractional free volume (F_v) as a function of CeO_2 nanoparticle concentration is as shown in Fig. 5c. From Fig. 5c, it is observed that the fractional free volume (F_v) of PVB/CeO_2 polymer nanodielectrics is exponentially decreasing as a function of CeO_2 nanoparticle concentration. This is due to hindrance to the molecular mobility of PVB polymer due to increased agglomeration of CeO_2 nanofiller [22].

4.6 X-ray diffraction results

The extensive studies on polymer crystallization in the presence of inorganic nanoparticles can be found in the literature [22, 35]. The crystalline domain in polymer nanodielectric materials may not alter much with the addition of nanoparticles. However, the presence of inorganic nanoparticles acts as nucleating agents and promotes molecular ordering in the amorphous domains of the polymer nanodielectrics [5]. The crystallinity of many polymer nanocomposites is increased with the addition of inorganic nanoparticles [22]. However, the crystallinity of some polymer nanocomposites shows decreasing trend [5]. In the present study the PVB/CeO_2 polymer nanodielectrics are crystalline in nature. The X-ray

diffraction measurements have been performed to examine crystallinity (χ_c) of the PVB/CeO_2 polymer nanodielectrics. Usually, the polymer consists of both crystalline as well as amorphous regions. The crystalline regions are generally represented by high-intensity sharp peaks. The low intense broad peaks are associated with the amorphous regions [36].

The deconvolution of crystalline peaks from the XRD spectrum was done by making use of PeakFit 4.1 software. The crystalline peaks were Gaussian fitted until the regression coefficient (R^2) value becomes 0.99. The percentage of crystallinity (χ_c) of PVB/CeO_2 polymer nanodielectrics are evaluated as $\chi_c(\%) = \frac{A_c}{A_t} \times 100$ where 'A_c' and 'A_t' are the area of the crystalline peaks and total area, respectively.

From Fig. 6a, it is observed that pure PVB shows a sharp crystalline peak at $2\theta = 20.42°$. The additional peaks have appeared at $2\theta = 20.68°$, 28.68°, 47.63°, and 56.51° in the XRD spectrum of PVB/CeO_2 polymer nanodielectrics for 0.2 wt% of CeO_2 nanofiller loading. Numerically, the crystallinity (χ_c) fluctuates within the error bar exhibiting constant values up to 0.8 wt% of CeO_2 nanofiller loading. This suggests that there is no appreciable change in the crystallinity (χ_c) of PVB/CeO_2 polymer nanodielectrics up to 0.8 wt% of CeO_2 nanofiller loading. The crystalline peak intensity at $2\theta = 20.68°$ in the XRD spectrum of PVB/CeO_2 polymer nanodielectrics is relatively higher for 1.0 wt% of CeO_2 nanofiller loading. This is the consequence of the increased crystallinity (χ_c) of PVB/CeO_2 polymer nanodielectrics. The mean crystallite size of pure PVB and PVB/CeO_2 polymer nanodielectrics have been estimated using basic Debye–Scherrer's equation [37].

$$D = \frac{K\lambda}{\beta\cos\theta} \tag{7}$$

where 'D' is the average crystallite size, 'λ' is the X-ray wavelength, 'β' is the width of the X-ray peak on the 2θ axis, normally measured as full width at half maximum (FWHM) after the error since instrumental broadening has been properly corrected, 'θ' is the Bragg angle, and 'K' is the so-called Scherrer constant. K depends on the crystallite shape and the size distribution, indices of the diffraction line, and the actual definition used for 'β'whether FWHM or integral breadth [38]. K can have values anywhere from 0.62 and 2.08. In this paper, $K = 0.94$ was used. Further, microstrain in the crystallite or nanocrystal

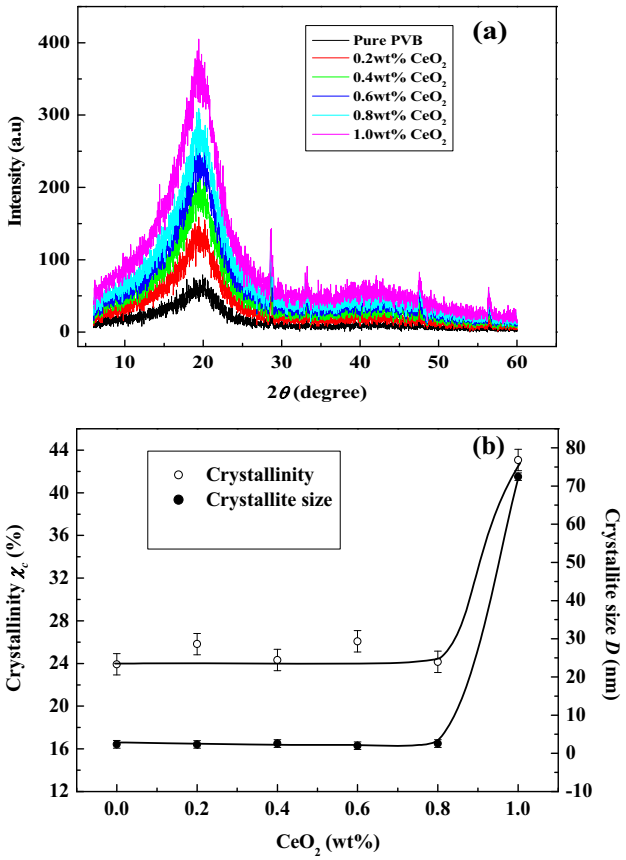

Fig. 6 **a** XRD spectra of pure PVB and PVB/CeO_2 nanodielectrics as a function of CeO_2 nanofiller wt%. **b** The variation of percentage of crystallinity (χ_c) and crystallite size (D) of PVB/CeO_2 polymer nanodielectrics as a function of CeO_2 nanoparticle wt%

also affects the width 'β' which needs to be considered in an accurate analysis. Spatial fluctuations in the alloy composition can also affect the width. The discussion on the accuracy of Eq. (7) can be found in the literature [38].

In the present study, the evaluated crystallinity (χ_c) and crystallite size (D) for pure PVB is 23.92% and 2.37 nm, respectively. The variation of percentage of crystallinity (χ_c) and crystallite size (D) of PVB/CeO_2 polymer nanodielectrics as a function of CeO_2 nanoparticle concentration is as shown in Fig. 6b and values are tabulated in Table 2 [39]. The PVB/CeO_2 polymer nanodielectrics doped with 1.0 wt% CeO_2 nanofiller show maximum crystallinity ($\chi_c = 43.07\%$) and crystallite size ($D = 72.44$ nm). The increased crystallinity of PVB/CeO_2 polymer nanodielectrics for 1.0 wt% of CeO_2 nanofiller loading can be explained as below.

Table 2 XRD results of PVB/CeO_2 polymer nanodielectrics

sWt% of CeO_2 nanoparticle	Crystallinity (χ_c) (%) ± 1%	Average crystallite size (D) ± 1 nm
0.0	23.92	2.37
0.2	25.82	2.33
0.4	24.32	2.58
0.6	26.08	2.01
0.8	24.15	2.58
1.0	43.07	72.44

As PVB is an admixture of polyvinyl and butyral groups [11] the CeO_2 nanoparticles may adsorb to the side chains of PVB to block the crystallization [40]. Therefore, the crystallinity (χ_c) and crystallite size (D) do not show any significant change in PVB/CeO_2 polymer nanodielectrics up to 0.8 wt% of CeO_2 nanofiller loading. The PVB/CeO_2 polymer nanodielectrics show a relatively higher value of crystallinity (χ_c) and crystallite size (D) for 1.0 wt% of CeO_2 nanofiller loading. The mobility of the PVB chain is severely restricted in PVB/CeO_2 polymer nanodielectrics for 1.0 wt% of CeO_2 nanofiller loading. This would facilitate the ordered arrangement of PVB chains. Consequently, the crystallinity (χ_c) and crystallite size (D) of PVB/CeO_2 polymer nanodielectrics show increased value for 1.0 wt% of CeO_2 nanofiller loading.

4.7 AC conductivity results of PVB/CeO_2 polymer nanodielectrics

The polymer–nanofiller interface and polymer amorphous phase provide pathways for ionic conduction [41]. Therefore, one can get greater insight about the polymer nanodielectrics by applying AC electric field. The variation of AC conductivity (σ_{ac}) of PVB/CeO_2 polymer nanodielectrics as a function of frequency is as shown in Fig. 7a. The AC conductivity of PVB/CeO_2 polymer nanodielectrics increases continuously as a function of frequency of the applied field. This is due to involvement of bound charge carriers and ionic hopping mechanism in the conduction process [42]. The variation of AC conductivity (σ_{ac}) and free volume (V_f) as a function of CeO_2 nanofiller concentration is as shown in Fig. 7b. The AC conductivity (σ_{ac}) of pure PVB at 5 MHz frequency is ($9.02 \times 10^{-6} \pm 0.48 \times 10^{-6}$) S/cm. The AC conductivity (σ_{ac}) of PVB/CeO_2 polymer nanodielectrics is decreased continuously as a function of CeO_2 nanoparticle loading. The minimum AC conductivity (σ_{ac}) is observed for 1.0 wt% of CeO_2 nanoparticle loading at 5 MHz frequency. The AC conductivity (σ_{ac}) of PVB/CeO_2 polymer nanodielectrics decreases three orders of magnitude (from $9.02 \times 10^{-6} \pm 0.48 \times 10^{-6}$ to $5.35 \times 10^{-9} \pm 0.26 \times 10^{-9}$ S/cm) for 1.0 wt% of CeO_2 nanoparticle loading at 5 MHz frequency. This is due to blocking of the conduction path for the ionic movement by the increased concentration of CeO_2 nanoparticles [43]

According to Jonscher power law, the AC conductivity $\sigma_{ac}(\omega)$ of many amorphous materials is directly proportional to the frequency of applied field and is given by $\sigma_{ac}(\omega) = A\omega^s$. Here, '$A$' is a pre-exponential factor and 'S' is the frequency exponent. The microscopic conduction mechanism of disordered systems is governed by two physical processes. They are classical hopping and quantum mechanical tunneling of charge carriers and ions. The two energetically favorable centers are in random distribution due to potential barrier separation [44]. The hopping of charge carriers and ions from one site to another is promoted by the free volume available in the polymeric systems [45]

The microscopic origin of the AC conductivity relaxation mechanism in disordered polymer nanodielectrics is explained by evaluating frequency exponent 'S'. The value of 'S' at room temperature for pure PVB and PVB/CeO_2 polymer nanodielectrics are evaluated using the slope of ln (σ_{ac}) vs ln ($2\pi f$) plot as shown in Fig. 7c. At room temperature the 'S' value in variety of disordered materials lies between $0.5 < S < 1$ [45]. The (S) values evaluated for pure PVB and PVB/CeO_2 polymer nanodielectrics lie between 0.54 and 0.79. This suggests that the observed behavior of AC conductivity with frequency obeys Jonscher power law for all concentration of CeO_2 nanoparticles at room temperature [46]. The variation of frequency exponent (S) and free volume (V_f) as a function of CeO_2 nanoparticle concentration is as shown in Fig. 7d. It is clear from Fig. 7d that frequency exponent (S) and free volume (V_f) exhibit exactly the opposite behavior.

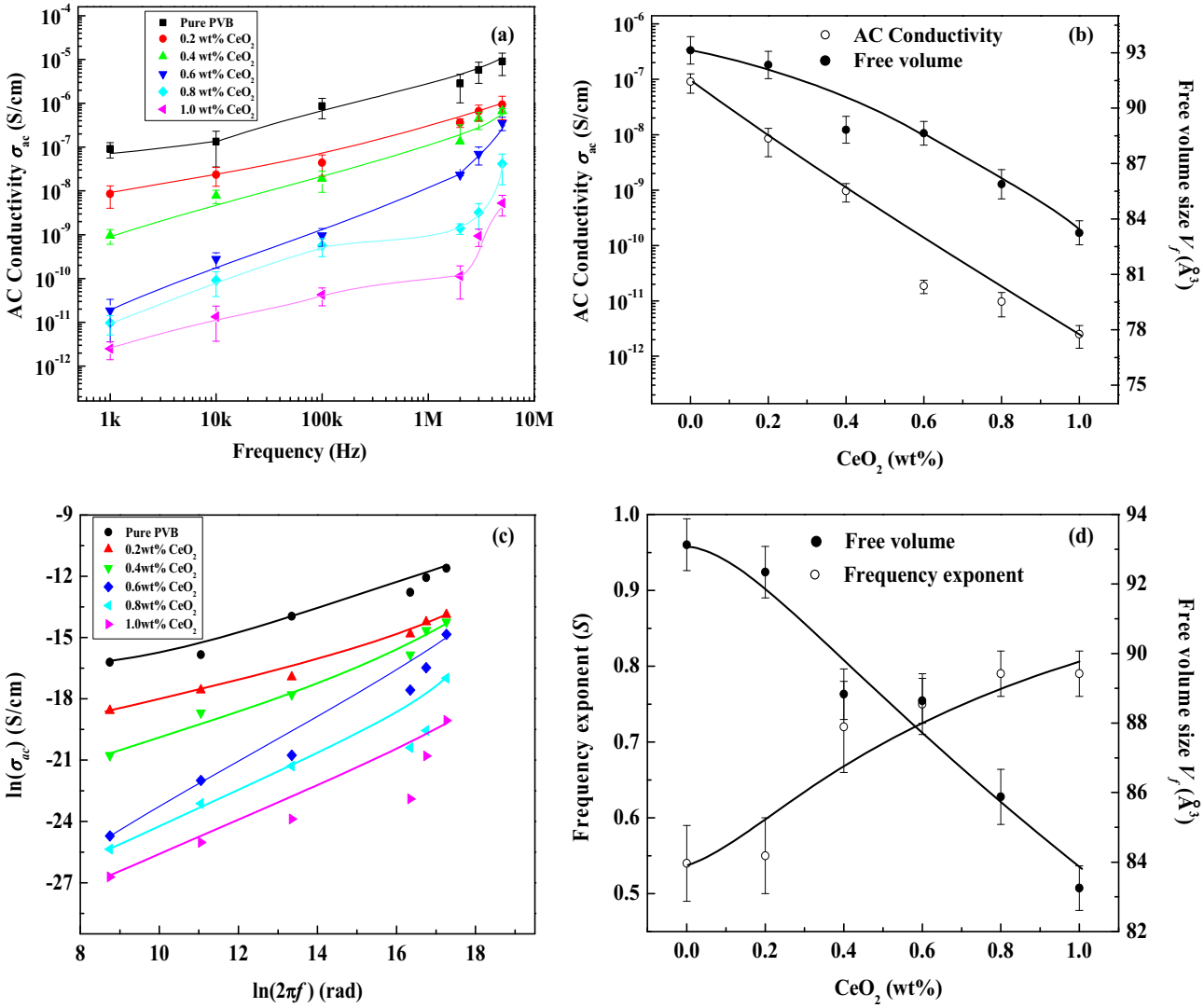

Fig. 7 The variation of **a** AC conductivity (σ_{ac}) as a function of applied frequency. **b** AC conductivity (σ_{ac}) and free volume size (V_f) as a function of CeO_2 nanoparticle wt%. **c** ln (σ_{ac}) vs ln ($2\pi f$) and **d** frequency exponent (S) of PVB/CeO_2 polymer nanodielectrics as a function of CeO_2 nanoparticle wt%

4.8 Dielectric results of PVB/CeO_2 polymer nanodielectrics

The dielectric constant of a polymer is mainly influenced by two parameters. One is change in molecular polarizability by modifying the type and number of polarizable groups and secondly the free volume associated with the polymer. Besides polarizability, dielectric losses are also an important feature of the dielectric material. The polarizability and dielectrics loss are due to the motion of bound charges in response to the applied electric field [47].

The variation of dielectric constant (ε') and free volume size (V_f) of PVB/CeO_2 polymer nanodielectrics as a function of CeO_2 nanofiller concentration is as shown in Fig. 8a. The dielectric constant of pure PVB at 1 kHz frequency is 16.90 ± 0.38. The dielectric constant (ε') is decreased to 11.36 ± 0.36 for 1.0 wt% of CeO_2 nanoparticle loading. The dielectric constant (ε') of PVB/CeO_2 polymer nanodielectrics is decreased continuously as a function of CeO_2 nanofiller loading. The decreased dielectric constant (ε') for the increased addition of CeO_2 nanoparticles is attributed to the hindrance to polymeric chain mobility at the bulk of PVB/CeO_2 polymer nanodielectrics [48]. The variation of dielectric constant (ε') of PVB/CeO_2 polymer nanodielectrics as a function of CeO_2 nanofiller concentration and frequency is as shown in Fig. 8b. In the low frequency region, there is a tendency of dipoles to

orient themselves in the direction of the applied electric field [49, 50]. This contributes to a higher dielectric constant (ε') of PVB/CeO_2 polymer nanodielectrics. The dielectric constant decreases with the increasing frequency of PVB/CeO_2 nanodielectrics. The decreased dielectric constant (ε') at the higher frequency region can be attributed to the interfacial polarization and decreased dipole mobility [51]. The interfacial polarization occurs due to the confinement of the charge carrier at the interface. The movement of charge carriers and ions accumulation requires a relatively long time during interfacial polarization [52].

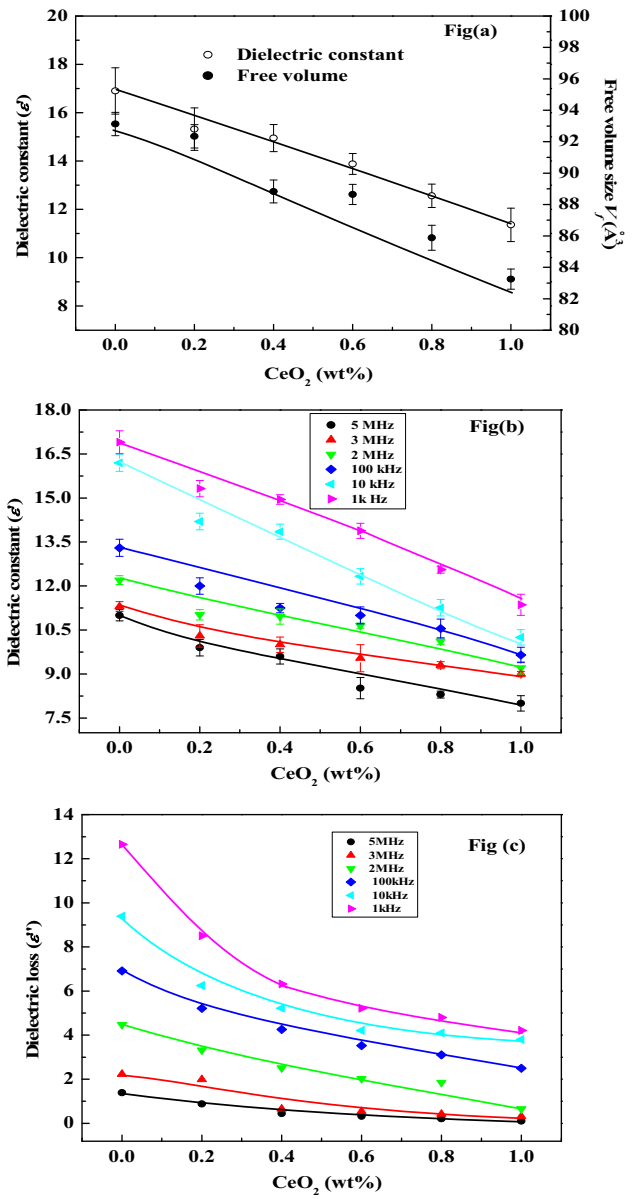

Fig. 8 **a** The variation of dielectric constant (ε') and free volume size (V_f) as a function of CeO_2 nanoparticle wt%. **b** Dielectric constant (ε') and **c** dielectric loss (ε'') of PVB/CeO_2 polymer nanodielectrics as a function of CeO_2 nanoparticle wt% and frequency of the applied field

In general, the dielectric loss in polymer nanodielectrics takes place due to the AC conductivity or ion jump, dipole relaxation, and interfacial polarization [13]. The ceramic particles normally display lower dissipation at a given frequency [53]. The variation of dielectric loss (ε'') of PVB/CeO_2 polymer nanodielectrics as a function of CeO_2 nanofiller loading is as shown in Fig. 8c. Both dielectric constant (ε') and dielectric loss (ε'') of PVB/CeO2 polymer nanodielectrics exhibit identical behavior for all concentrations of CeO2 nanoparticle loading for the entire range of frequency (from 1 kHz to 5 MHz). The dielectric loss (ε'') of pure PVB at 1 kHz frequency is 12.65. The minimum dielectric loss (ε'') of 4.21 is observed in PVB/CeO_2 polymer nanodielectrics for 1.0 wt% of CeO_2 nanoparticle loading. This suggests that the influence of interface polarization on the dielectric loss becomes less significant for 1.0 wt% of CeO_2 nanoparticle loading.

4.9 Scanning electron microscopy results

Scanning electron microscopy is a convenient technique used for the investigation of the surface morphology of polymers. The dispersion and distribution of nanoparticles in the polymer matrix play a decisive role in predicting the bulk properties. The SEM micrographs of pure PVB and PVB/CeO_2 polymer nanodielectrics with increased CeO_2 nanoparticle concentration are as shown in Fig. 9a–f.

From the SEM images, it is observed that pure PVB exhibits homogeneous smooth surface, whereas in PVB/CeO_2 polymer nanodielectrics show relatively rough. In the SEM images of PVB/CeO2 polymer nanodielectrics for 0.2 and 0.4 wt% of CeO_2 nanoparticles loading uniformly distributed CeO_2 nanoparticles throughout the PVB matrix can be seen. The SEM images of PVB/CeO_2 polymer nanodielectrics show nanoclusters of irregular shapes for 0.6, 0.8, and 1 wt% of CeO_2 nanoparticle loading. The CeO_2 nanoparticles exhibit greater tendency to undergo self-agglomeration in the host polymer matrix. Due to high aspect ratio, the agglomeration of CeO_2 nanoparticles leads to the formation of nanoclusters of irregular shapes in the PVB matrix [5].

5 Correlation between free volume parameters, SEM, and XRD results with AC conductivity and dielectric properties of PVB/CeO_2 polymer nanodielectrics

The free volume and crystallinity (χ_c) are the essential parameters to investigate the microstructure of the polymer nanodielectrics. The free volume size (V_f), AC conductivity (σ_{ac}), and dielectric properties of PVB/CeO_2 polymer nanodielectrics exhibit identical trends. The crystallinity (χ_c) shows opposite behavior with respect to free volume as a function of CeO_2 nanoparticle concentration. The free volume size (V_f) and AC conductivity of PVB/CeO_2 polymer nanodielectrics are decreased continuously as a function of CeO_2 nanoparticle concentration. This is due to the blocking of the conduction path for the ionic movement in the PVB polymeric matrix. The mobility of the PVB chain is much more reduced for 1.0 wt% of CeO_2 nanoparticle loading. Therefore, the free volume size (V_f) and AC conductivity show minimum value and maximum crystallinity for 1.0 wt% of CeO_2 nanoparticle loading. The increased incorporation of

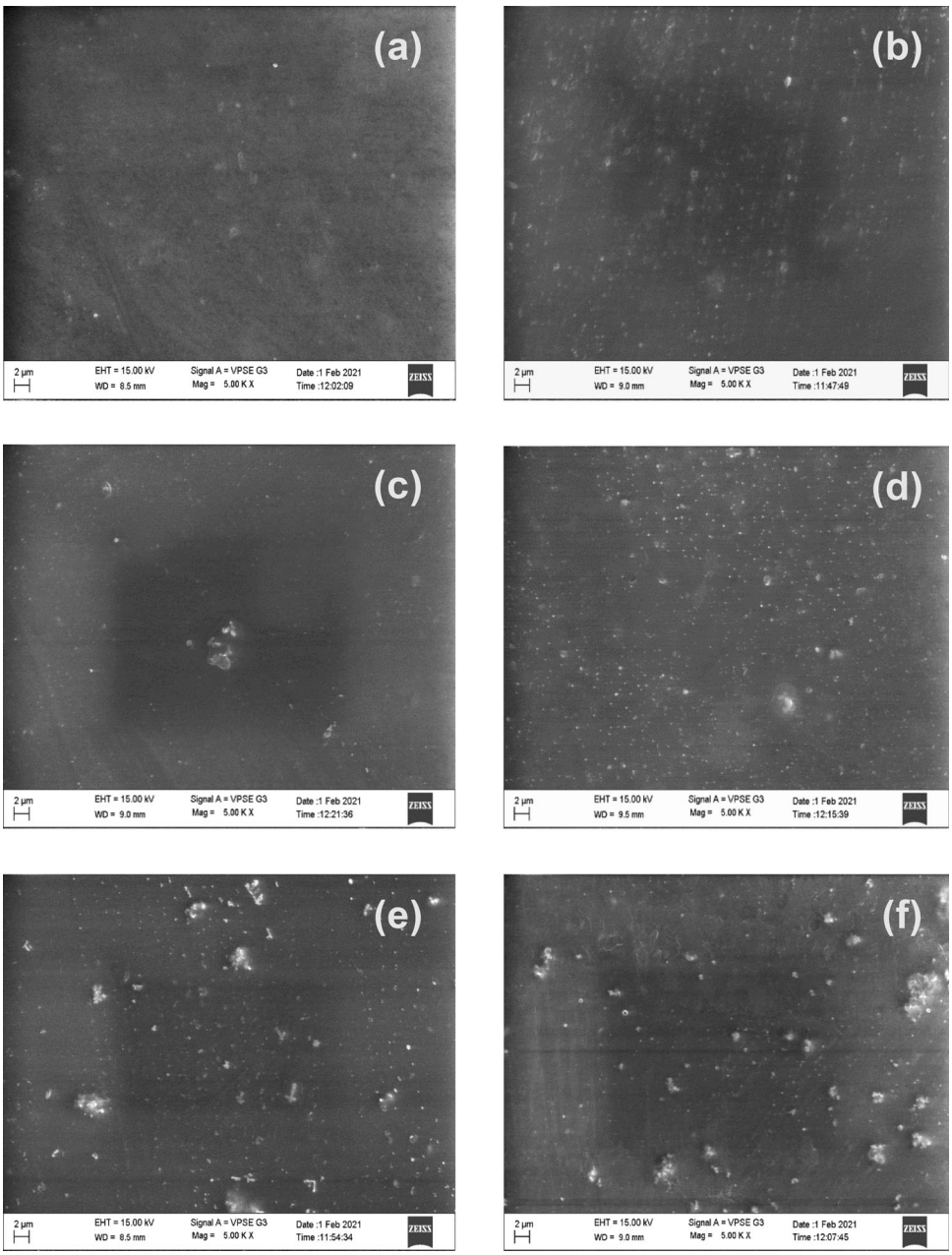

Fig. 9 SEM images of **a** pure PVB, **b** PVB + 0.2 wt% CeO_2, **c** PVB + 0.4 wt% CeO_2, **d** PVB + 0.6 wt% CeO_2, **e** PVB + 0.8 wt% CeO_2, and **f** PVB + 1.0 wt% CeO_2 polymer nanodielectrics

CeO_2 nanoparticles promotes crystallization of PVB matrix and hence the crystallinity (χ_c).

The dielectric constant of polymer nanodielectrics solely depends on the extent of polarization of polymer. The polarizable groups present in the PVB matrix interact with incorporated nanofillers. The alignment of these polarizable groups is restricted due to decreased free volume. In the lower frequency region, there is enough time for the proper alignment of dipoles. This results in a maximum dielectric constant of PVB/CeO_2 polymer nanodielectrics at lower frequency regions. At higher frequencies, the response of the polar group of PVB is delayed with respect to an oscillating electric field. This is due to the inability of dipoles to co-operate with the electric field. This is the reason for the gradual reduction of the dielectric constant of PVB/CeO_2 polymer nanodielectrics at a higher frequency region.

6 Summary and conclusion

Based on the above experimental results following conclusions are drawn:

1. The o-Ps lifetime (τ_3) and free volume size (V_f) of PVB/CeO_2 polymer nanodielectrics show minimum value for 1.0 wt% of CeO_2 nanoparticle loading. The chemical interaction between CeO_2 nanoparticles with PVB side chains restricts the molecular mobility of PVB polymer. The o-Ps intensity (I_3) is reduced drastically for 0.2 wt% of CeO_2 nanoparticle loading. The presence of CeO_2 nanoparticles and polar groups of PVB inhibits the o-Ps formation.
2. The ordered arrangement of PVB chains is not much affected at lower wt% of CeO_2 nanoparticle loading. The higher concentration of CeO_2 nanoparticle loading promotes crystallization of PVB matrix and hence the crystallinity (χ_c) in PVB/CeO_2 polymer nanodielectrics.
3. The SEM images show uniform dispersion of CeO_2 nanoparticles for lower concentration of CeO_2 nanoparticle loading. The CeO_2 nanoparticles agglomeration leads to the formation of nanoclusters of irregular shapes in the PVB polymer matrix for higher concentration of CeO_2 nanoparticle loading.
4. The reduced free volume restricts the ionic mobility of CeO_2 nanoparticles and hence the AC conductivity (σ_{ac}) in PVB/CeO_2 polymer nanodielectrics for higher wt% of CeO_2 nanoparticle loading. The AC conductivity obeys Jonscher power law for all concentration of CeO_2 nanoparticles loading at room temperature.
5. The decreased dielectric constant (ε') is due to hindrance to the alignment of polarizable groups in PVB/CeO_2 polymer nanodielectrics for higher concentration of CeO_2 nanofiller loading.

Acknowledgements

One of the authors M. Raghavendra is grateful to the University of Mysore, Mysuru for providing a Junior Research Fellowship (JRF) to carry out this research work.

References

1. S. Singha, M.J. Thomas, Influence of filler loading on dielectric properties of epoxy-Zno nanocomposites. IEEE Trans. Dielectr. Electr. Insul. **16**, 531–542 (2009). https://doi.org/10.1109/TDEI.2009.4815189
2. M.F. Fréchette, C.W. Reed, The role of molecular dielectrics in shaping the interface of polymer nanodielectrics, in *Annu. Rep.—Conf. Electr. Insul. Dielectr. Phenomena, CEIDP*, vol. 2 (2007), pp. 279–285. https://doi.org/10.1109/CEIDP.2007.4451618.
3. J. Keith Nelson, in *Dielectric Polymer Nanocomposites*, ed. by J. Keith Nelson (Springer, New York, 2011), p. 30 https://doi.org/10.1007/978-1-4419-1591-7.
4. C. Zhang, G.C. Stevens, The dielectric response of polar and non-polar nanodielectrics. IEEE Trans. Dielectr. Electr. Insul. **15**, 606–617 (2008). https://doi.org/10.1109/TDEI.2008.4483483
5. S. Ningaraju, A.P. Gnana Prakash, H.B. Ravikumar, Studies on free volume controlled electrical properties of PVA/NiO and PVA/TiO_2 polymer nanocomposites. Solid State Ionics **320**, 132–147 (2018). https://doi.org/10.1016/j.ssi.2018.03.006
6. J. Hu, Y. Zhou, X. Sheng, Optical diffusers with enhanced properties based on novel polysiloxane@CeO_2@PMMA fillers. J. Mater. Chem. C. **3**, 2223–2230 (2015). https://doi.org/10.1039/c4tc02287d
7. T.B. Atisme, C.Y. Yu, E.N. Tseng, Y.C. Chen, P.K. Hsu, S.Y. Chen, Interface interactions in conjugated polymer composite with metal oxide nanoparticles. Nanomaterials **9**, 1–12 (2019). https://doi.org/10.3390/nan0o9111534

8. S. Pizzanelli, D. Prevosto, M. Labardi, T. Guazzini, S. Bronco, C. Forte, L. Calucci, Dynamics of poly(vinyl butyral) studied using dielectric spectroscopy and 1H NMR relaxometry. Phys. Chem. Chem. Phys. **19**, 31804–31812 (2017). https://doi.org/10.1039/c7cp02595e
9. P. Kumar, N. Khan, D. Kumar, Polyvinyl Butyral (PVB), Versetile template for designing nanocomposite/composite materials: a review. Green Chem. Technol. Lett. **2**, 185–194 (2016). https://doi.org/10.18510/gctl.2016.244
10. K. Nakane, T. Kurita, T. Ogihara, N. Ogata, Properties of poly(vinyl butyral)/TiO_2 nanocomposites formed by sol-Gel process. Compos. B **35**, 219–222 (2004). https://doi.org/10.1016/S1359-8368(03)00066-0
11. S. Gupta, S. Seethamraju, P.C. Ramamurthy, G. Madras, Polyvinylbutyral based hybrid organic/inorganic films as a moisture barrier material. Ind. Eng. Chem. Res. **52**, 4383–4394 (2013). https://doi.org/10.1021/ie3022412
12. Y. Akinay, F. Hayat, B. Çolak, Absorbing properties and structural design of PVB/Fe_3O_4 nanocomposite. Mater. Chem. Phys. **229**, 460–466 (2019). https://doi.org/10.1016/j.matchemphys.2019.03.039
13. P.J. Bora, I. Azeem, K.J. Vinoy, P.C. Ramamurthy, G. Madras, Morphology controllable microwave absorption property of polyvinylbutyral (PVB)-MnO_2 nanocomposites. Compos. B **132**, 1–24 (2018). https://doi.org/10.1016/j.compositesb.2017.09.014
14. Y. Su, M. Zhou, G. Sui, J. Lan, H. Zhang, X. Yang, Polyvinyl butyral composites containing halloysite nanotubes/reduced graphene oxide with high dielectric constant and low loss. Chem. Eng. J. **394**, 124910 (2020). https://doi.org/10.1016/j.cej.2020.124910
15. A. Mandal, S. Mukherjee, S. Pan, A. Sengupta, Positron lifetime measurements in natural rubber with different fillers. Int. J. Mod. Phys. Conf. Ser. **22**, 112–117 (2013). https://doi.org/10.1142/s2010194513009999
16. H.B. Ravikumar, C. Ranganathaiah, G.N. Kumaraswamy, S. Thomas, Positron annihilation and differential scanning calorimetric study of poly(trimethylene terephthalate)/EPDM blends. Polymer **46**, 2372–2380 (2005). https://doi.org/10.1016/j.polymer.2004.12.058
17. P. Kirkegaard, N.J. Pedersen, M. Eldrup, PATFIT-88: a data processing system for positron annihilation spectra on mainframe and personal computers, 1989.
18. H. Nakanishi, S.J. Wang, Y.C. Jean, *Positron Annihilation in Fluids*, Sharma. (World Scientific, Singapore, 1988), pp. 292–293
19. S.J. Tao, Positronium annihilation in molecular substances. J. Chem. Phys. **56**, 5499–5510 (1972). https://doi.org/10.1063/1.1677067
20. M. Eldrup, D. Lightbody, J.N. Sherwood, The temperature dependence of positron lifetimes in solid pivalic acid. Chem. Phys. **63**, 51–58 (1981). https://doi.org/10.1016/0301-0104(81)80307-2
21. Y.C. Jean, Positron annihilation spectroscopy for chemical analysis: A novel probe for microstructural analysis of polymers. Microchem. J. **42**, 72–102 (1990). https://doi.org/10.1016/0026-265X(90)90027-3
22. S. Ningaraju, K. Jagadish, S. Srikantaswamy, A.P. Gnana Prakash, H.B. Ravikumar, Synthesis of graphite oxide nanoparticles and conductivity studies of PSF/GO and PSAN/GO polymer nanocomposites. Mater. Sci. Eng. B. **246**, 62–75 (2019). https://doi.org/10.1016/j.mseb.2019.06.002
23. J. Bergström, *Mechanics of Solid Polymers: Theory and Computational Modeling*, 1st edn. (Moffett Field, Matthew Deans, 2015), pp. 1–499
24. K.S. Hemalatha, K. Rukmani, Synthesis, characterization and optical properties of polyvinyl alcohol-cerium oxide nanocomposite films. RSC Adv. **6**, 74354–74366 (2016). https://doi.org/10.1039/c6ra11126b
25. M. Elango, M. Deepa, R. Subramanian, G. Saraswathy, Investigation of structural, morphological and antimicrobial properties of polyindole/Ag doped CeO_2 nanocomposites. Mater. Today Proc. **26**, 3544–3551 (2019). https://doi.org/10.1016/j.matpr.2019.07.246
26. G. Dlubek, M. Stolp, C. Nagel, H.M. Fretwell, M.A. Alam, H.J. Radusch, Effect of crystallization and of water uptake on the free-volume hole size in polyamides 6 and 66. J. Phys. Condens. Matter. **10**, 10443–10450 (1998). https://doi.org/10.1088/0953-8984/10/46/012
27. H.A. Hristov, B. Bolan, A.F. Yee, L. Xie, D.W. Gidley, Measurement of hole volume in amorphous polymers using positron spectroscopy. Macromolecules **29**, 8507–8516 (1996). https://doi.org/10.1021/ma960719k
28. S. Awad, H. Chen, G. Chen, X. Gu, J.L. Lee, E.E. Abdel-Hady, Y.C. Jean, Free volumes, glass transitions, and cross-links in zinc oxide/waterborne polyurethane nanocomposites. Macromolecules **44**, 29–38 (2011). https://doi.org/10.1021/ma102366d
29. P. Winberg, K. DeSitter, C. Dotremont, S. Mullens, I.F.J. Vankelecom, F.H.J. Maurer, Free volume and interstitial mesopores in silica filled poly(1-trimethylsilyl-1-propyne) nanocomposites. Macromolecules **38**, 3776–3782 (2005). https://doi.org/10.1021/ma047369j
30. M. Iwan, T. Andryszewski, M. Wydryszek, M. Fialkowski, Fabrication of nanocomposites by covalent bonding between noble metal nanoparticles and polymer matrix. RSC Adv. **5**, 70127–70138 (2015). https://doi.org/10.1039/c5ra12474c
31. P. Min, S. Zhang, Y. Xu, R. Li, Enhanced oxygen storage capacity of CeO_2 with doping- induced unstable crystal

structure. Appl. Surf. Sci. **448**, 435–443 (2018). https://doi.org/10.1016/j.apsusc.2018.04.103
32. Y.Y. Wang, H. Nakanishi, Y.C. Jean, T.C. Sandreczki, M. Douglas, Positron annihilation in Amine-cured epoxy polymers- pressure dependence. J. Polym. Sci. **28**, 1431–1441 (1990)
33. S. El-Gamal, M. Elsayed, Positron annihilation and electrical studies on the influence of loading magnesia nanoribbons on PVA-PVP blend. Polym. Test. **89**, 106681 (2020). https://doi.org/10.1016/j.polymertesting.2020.106681
34. G. Xue, J. Zhong, S. Gao, B. Wang, Correlation between the free volume and thermal conductivity of porous poly(vinyl alcohol)/reduced graphene oxide composites studied by positron spectroscopy. Carbon N. Y. **96**, 871–878 (2016). https://doi.org/10.1016/j.carbon.2015.10.041
35. A. Jabbarzadeh, B. Halfina, Unravelling the effects of size, volume fraction and shape of nanoparticle additives on crystallization of nanocomposite polymers. Nanoscale Adv. **1**, 4704–4721 (2019). https://doi.org/10.1039/c9na00525k
36. J.H. Kim, Y.M. Lee, Gas permeation properties of poly(-amide-6-b-ethylene oxide)-silica hybrid membranes. J. Memb. Sci. **193**, 209–225 (2001). https://doi.org/10.1016/S0376-7388(01)00514-2
37. P. Scherrer, Bestimmung der Grösse und der inneren Struktur von Kolloidteilchen mittels Röntgenstrahlen. Nachr. Ges. Wiss. Göttingen **26**, 98 (1918)
38. J.I. Langford, A.J.C. Wilson, Scherrer after Sixty years: a survey and some new results in the determination of crystallite size. J. Appl. Cryst. **11**, 102 (1978)
39. E. Kavya Valsan, A. John, M. Raghavendra, H.B. Ravikumar, Free Volume Controlled Ionic Conductivity in Poly Vinyl Alcohol/Zinc Acetate Solid Polymer Electrolytes. J. Electrochem. Soc. **167**, 060525 (2020). https://doi.org/10.1149/1945-7111/ab861e
40. H. Papananou, E. Perivolari, K. Chrissopoulou, S.H. Anastasiadis, Tuning polymer crystallinity via the appropriate selection of inorganic nanoadditives. Polymer **157**, 111–121 (2018). https://doi.org/10.1016/j.polymer.2018.10.018
41. P. Utpalla, S.K. Sharma, K. Sudarshan, V. Kumar, P.K. Pujari, Free volume correlation with ac conductivity and thermo-mechanical properties of poly (ethylene oxide)-silica nanocomposites. Eur. Polym. J. **117**, 10–18 (2019). https://doi.org/10.1016/j.eurpolymj.2019.04.049
42. S.R. Elliott, Ac conduction in amorphous chalcogenide and pnictide semiconductors. Adv. Phys. **36**, 135–218 (1987). https://doi.org/10.1080/00018738700101971
43. R. Nangia, N.K. Shukla, A. Sharma, Dielectric relaxation and AC conductivity behaviour of $Se_{80}Te_{15}Bi_5$/PVA nanocomposite film. Polym. Test. **79**, 106088 (2019). https://doi.org/10.1016/j.polymertesting.2019.106088
44. N. Parvatikar, M.V.N. Ambika Prasad, Frequency-dependent conductivity and dielectric permittivity of polyaniline/CeO_2 composites. J. Appl. Polym. Sci. **100**, 1403–1405 (2006). https://doi.org/10.1002/app.22950
45. K.V.A. Kumar, M. Raghavendra, V.N. Hegde, A.P.G. Prakash, H.B. Ravikumar, Gamma irradiation induced microstructural modification and electrical conductivity of bakelite resistive plate chamber material. J. Radioanal. Nucl. Chem. (2021). https://doi.org/10.1007/s10967-020-07565-z
46. M. Tripathi, P. Chawla, CeO_2-TiO_2 photoanode for solid state natural dye-sensitized solar cell. Ionics **21**, 541–546 (2015). https://doi.org/10.1007/s11581-014-1172-6
47. E. Tuncer, A.J. Rondinone, J. Woodward, I. Sauers, D.R. James, A.R. Ellis, Cobalt iron-oxide nanoparticle modified poly(methyl methacrylate) nanodielectrics: dielectric and electrical insulation properties. Appl. Phys. A **94**, 843–852 (2009)
48. P.S. Anjana, M.T. Sebastian, M.N. Suma, P. Mohanan, Low dielectric loss PTFE/CeO_2 ceramic composites for microwave substrate applications. Int. J. Appl. Ceram. Technol. **5**, 325–333 (2008). https://doi.org/10.1111/j.1744-7402.2008.02228.x
49. S. Mahendia, A.K. Tomar, S. Kumar, Electrical conductivity and dielectric spectroscopic studies of PVA-Ag nanocomposite films. J. Alloys Compd. **508**, 406–411 (2010). https://doi.org/10.1016/j.jallcom.2010.08.075
50. M. Maria Lumina Sonia, S. Anand, S. Blessi, S. Pauline, A. Manikandan, Effect of surfactants (PVB/EDTA/CTAB) assisted sol-gel synthesis, structural, magnetic and dielectric properties of $NiFe_2O_4$ nanoparticles. Ceram. Int. **44**, 22068 (2018). https://doi.org/10.1016/j.ceramint.2018.08.317
51. Y. Su, G. Sui, J. Lan, X. Yang, A highly stretchable dielectric elastomer based on core-shell structured soft polymer-coated liquid-metal nanofillers. Chem. Commun. **56**, 11625 (2020). https://doi.org/10.1039/D0CC04224B
52. E. Kar, N. Bose, S. Das, N. Mukherjee, S. Mukherjee, Enhancement of electroactive β phase crystallization and dielectric constant of PVDF by incorporating GeO_2 and SiO_2 nanoparticles. Phys. Chem. Chem. Phys. **17**, 22784–22798 (2015). https://doi.org/10.1039/c5cp03975d
53. C. Jia, Z. Shao, H. Fan, J. Wang, Preparation and dielectric properties of cyanoethyl cellulose/$BaTiO_3$ flexible nanocomposite films. RSC Adv. **5**, 15283–15291 (2015). https://doi.org/10.1039/c4ra13960g